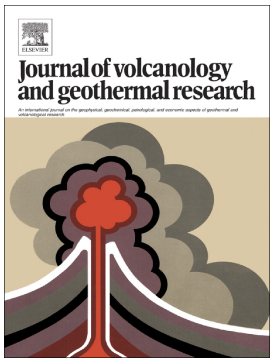

Sudden alteration in the seismic behavior of the Domuyo volcanic complex in the southern volcanic backarc zone, Argentina

Laura B. Godoy, Silvina Nacif, Andrés Nacif, Rodolfo Christiansen, Orlando Álvarez, Mario Gimenez, Andrés Folguera

PII: S0377-0273(23)00213-5

DOI: https://doi.org/10.1016/j.jvolgeores.2023.107956

Reference: VOLGEO 107956

To appear in: *Journal of Volcanology and Geothermal Research*

Received date: 14 June 2023

Revised date: 23 October 2023

Accepted date: 28 October 2023

Please cite this article as: L.B. Godoy, S. Nacif, A. Nacif, et al., Sudden alteration in the seismic behavior of the Domuyo volcanic complex in the southern volcanic backarc zone, Argentina, *Journal of Volcanology and Geothermal Research* (2023), https://doi.org/10.1016/j.jvolgeores.2023.107956

SUDDEN ALTERATION IN THE SEISMIC BEHAVIOR OF THE DOMUYO VOLCANIC COMPLEX IN THE SOUTHERN VOLCANIC BACKARC ZONE, ARGENTINA.

Godoy, Laura B.[1,2]; Nacif, Silvina[1,2]; Nacif, Andrés[2]; Christiansen, Rodolfo[4]; Álvarez, Orlando[1,2]; Gimenez, Mario[1,2]; Folguera, Andrés[3].

1 CONICET (Consejo Nacional de Investigaciones Científicas y Técnicas), Av. Rivadavia 1917, C1033AAJ, Argentina.

2 instituto Geofísico Sismológico F. Volponi, FCEFyN, Universidad Nacional de San Juan (UNSJ), Ruta 12 km 17 Marquesado, Rivadavia, San Juan, Argentina.

3 instituto de Estudios Andinos. Don Pablo Groeber, UBA – CONICET, Argentina.

4 Leibniz Institute for Applied Geophysics - LIAG - Stillweg 2, D-30655 Hannover, Germany.

KEYWORD. DOMUYO VOLCANIC COMPLEX; MICROSEISMICITY; FOCAL MECHANISM; CRUSTAL SEISMICITY

I. ABSTRACT

The Domuyo volcanic complex (DVC) and its geothermal field in the retroarc zone of the southern Central Andes of Argentina present reduced seismicity according to different catalogs (USGS and INPRES). However, in 2015/2016 a local project was carried out in the area to describe its seismo-volcanic activity, registering a large number of volcano-tectonic (VT) events (538 VT). Considering there is scarce information on these events, this study focuses on analyzing the Domuyo Volcanic Complex (DVC) to assess its seismicity. Therefore, we installed a local seismological network in the study area and compared results with data registered by other authors. Four seismological networks were used, to obtain a more precise location of the seismic events and calculate the focal mechanisms of earthquakes with magnitudes greater than 2. For the first record of crustal seismicity detected by INPRES the September 10th, 2016 with a Ml 3.3, we calculated the focal mechanism with two possible solutions: a thrust solution with a strike component and a favored normal solution with a strike

component. Additionally, we relocated the largest event in the Domuyo region on March 27th, 2019, with a magnitude of 4.4 (NEIC – USGS) and focal mechanism with a normal solution and a small strike component, obtaining a shallower depth of 3.9 km instead of 10 km. The new seismological data used in this paper, correspond to September 10th 2016, and two different time periods, the first comprising continuous data from March to April 2019, when the largest registered earthquake occurred in the Domuyo region, and the second from December 2019 to January 2021. At these periods, registered seismicity had magnitudes Ml between 1.9 to 2.8, and focal depths between 1.8 and 5.2 km. Four of these events count with focal mechanisms with extensional and limited strike-slip components that are tentatively linked to the known neotectonic structures affecting the western slope of the DVC. This seismic sequence agrees with previous proposals in which degasification from a magmatic body at shallow depths constitutes the trigger factor.

II. INTRODUCTION

The Domuyo volcanic complex (DVC) is a dome-caldera system with no historical effusive/explosive activity (Miranda et al., 2006). It is located in the backarc of the Southern Volcanic Zone (SVZ) in the Neuquén Province of Argentina (Stern, 2004), associated with the subduction of the Nazca oceanic plate below the South American plate with an east dipping angle of 30° (e.g., Farías et al., 2010; Tassara and Yañez, 2003). Since 2008 to the present several changes have been identified in the volcanic system, which can constitute potential indicators of volcanic unrest. In particular, a 12 to 15 cm/yr inflation (Lundgren et al., 2018; Astort et al., 2019) was determined by interferometric synthetic aperture radar (InSAR) data, which was explained through a tabular body model at a depth of about 6.5 km (Lundgren et al., 2020). Additionally, those authors detected thermal changes by satellite-based

thermal infrared (TIR) remote sensing. In addition, Tassi et al. (2016) found high values of R/Ra (6.8) in the fumaroles located on the western slope of the DVC, which indicates concentrations of mantle He^3, a product of the active degassing of a magmatic body at an unknown depth. In this line, Godoy et al. (2021) determined a thinner magnetized crust of around 5-6 km in this area when compared to 11 km thick to the south which doubles its thickness, implying higher thermal conditions in the backarc zone at the location of the DVC. All this evidence may indicate triggering mechanisms and alterations in the seismic behavior of the DVC after 2008.

The global (NEIC, USGS) and regional catalogs (INPRES, Argentina) show that the Domuyo volcanic complex, whose activity has been largely debated, shows no seismicity from 1973 to 2016 (Figure 1). However, since 2016, INPRES has reported seven crustal events (Figure 1C). On March 27th 2019, the USGS reported the highest event among these, which was felt by the nearby population (Figure 1C). Additionally, Godoy et al. (2021), using a local network, detected 538 volcano-tectonic events (magnitude range -1.5 to 1.5), at less than 8 km deep, which occurred from December 2015 to March 2016. These events were classified into two groups according to their depth. The shallower events (2-3 km) were related to the hydrothermal reservoir whereas the deeper ones (6-8 km) were most likely produced around the magma source. They can be interpreted as associated with pore pressure and hydrofracturing, and constitute an anomalous number of volcano-tectonic events in only 93 days. The analysis of these events was used to complement our results in this work.

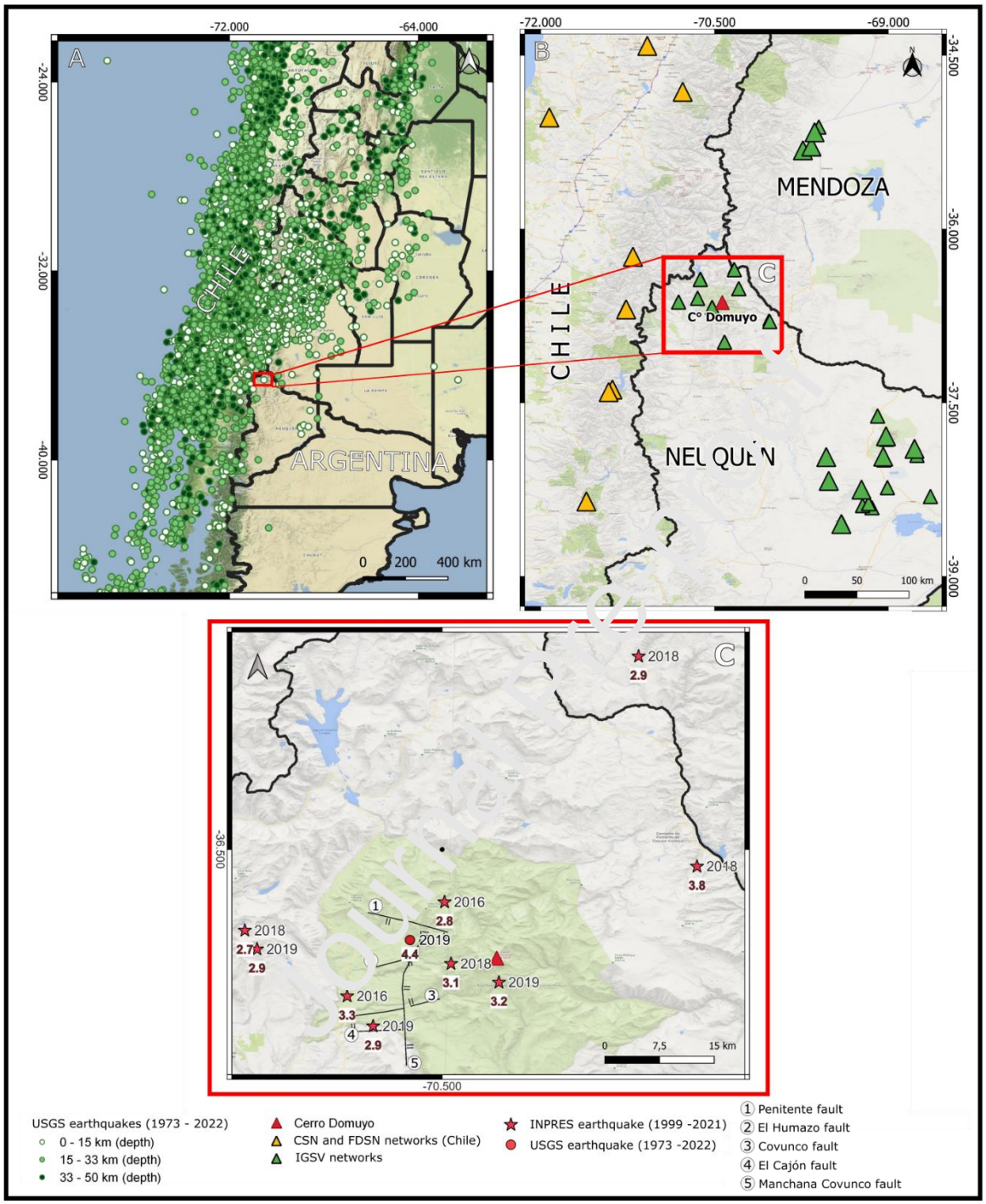

Figure 1. A) Image representation of southern South America which shows the interplate and intracrustal earthquakes at depths less than 50 km (NEIC Catalog, USGS). Crustal earthquakes by USGS, from 1973 to 2022, with a green scale representing the epicenter's depth. The red rectangle marks the study zone, noting only one earthquake in that area. B) Satellite TM image in which the triangles represent the stations used for the earthquake location. The green triangles are the temporal local networks from Instituto Geofísico Sismológico Ing Volponi (IGSV). The orange triangles mark the stations from Chile, the National Seismological Center of the University of Chile (CSN) network, and the Federation of Digital Seismograph Networks (FDSN). The Domuyo volcanic complex is represented by a red triangle. C)

Satellite image with the earthquakes from USGS and INPRES catalogs, the epicenters are represented with a circle and stairs, respectively. The numbers near the epicenters represent the year of occurrence (in white color) and the magnitude (in red color).

All the changes identified in the DVC imply instability in the magmatic/hydrothermal system from at least 2008 to 2020 (Tassi et al., 2016; Lundgren et al., 2018; Astort et al., 2019; Godoy et al. 2021). The IGSV catalog, available from 2010, was built from 4 local temporary seismological networks, 3 of them deployed in the south of Mendoza Province and the other in the center of Neuquén Province (Figure 1B). We used this catalog to verify the seismic activity in the Domuyo region. From 2010 to 2015 no earthquake activity in the Domuyo region was detected, being only detected from 2016 to 2020. In particular, from December 2019, after installing a local temporary broadband seismological network in the DVC, registering continuously for 13 months, evidence of increased seismic behavior was registered. This work analyzes the local seismicity of the DVC from the end of 2015 to the beginning of 2021, in order to establish possible links between this recent unrest period, the release of magmatic gases (Tassi et al., 2016), and the observed inflation (Lundgren et al., 2018; Astor et al., 2019, and d'Oreye et al., 2019).

III. GEOLOGICAL SETTING

The Domuyo volcanic complex (DVC) is a rhyolitic-dacitic dome-basaltic complex emplaced in a collapse caldera that intrudes a large anticline (Groeber, 1947; Llambías et al., 1978; Miranda et al., 2006; Folguera et al., 2007). This anticline exhumes the Permian-Triassic Choiyoi Group, which covers and intrudes a Carboniferous sedimentary succession at depth (Zöllner y Amos, 1973; Leanza et al., 2005; Llambías et al., 2007; Zappettini et al., 2012). Over this succession, deposits of Jurassic and Cenozoic ages are sparse in the region (Silva – Fragoso et al., 2021; Borghi et al., 2023). An eruptive initial period roughly ranging from 2.5 to 0.11 Ma was recognized, which consisted of two stages (Brousse and

Pesce, 1982; JICA, 1983; Pesce, 2013): the first stage, which covered the late Pliocene to the early Pleistocene, is characterized by a dominant calc-alkaline composition and widespread pyroclastic flows. The second stage, which occurred from the Middle to the Upper Pleistocene (Holocene?), is characterized by mafic flows and the development of monogenetic rhyolitic domes like Cerro Domo, Covunco Las Papas, and Bota Cura, to the southwest of the Cerro Domuyo. In addition, DVC is considered an important geothermal resource. Its geothermal field is located on the western slope of Cerro Domuyo (Llambías et al., 1978; JICA, 1983, 1984; Chiodini et al., 2014). This is a high enthalpy system controlled by faults, with fumaroles, shallow hot springs, and geysers. It was considered by Chiodini et al. (2014) to be the second-highest measured advective heat flux of any terrestrial hydrothermal system, after Yellowstone. Tassi et al. (2016) conducted a comprehensive study of the chemical and isotopic composition of water and gas, determining the origin of geothermal fluids. They made a model of the hydrothermal reservoir, and the patterns of fluid circulation in the geothermal field, and proposed two main water reservoirs at 0.4 and 2-3 km depth, respectively. These authors also found high values of R/Ra (6.81) in the fumaroles located on the western slope of Cerro Domuyo, indicating high values of mantle He^3, a product of the active degassing of a magmatic body at an unknown depth (Tassi et al., 2016).

The principal structure affecting the DVC is the Manchana Covunco fault, located on its western side (Figure 1). It is a north-south normal fault dipping to the east which constitutes the main structure controlling the geothermal field dynamics (Galetto et al., 2018). This structure shows evidence of neotectonic displacements affecting pumice materials emitted in the first phase of the DVC activity (Folguera et al., 2007). A series of fault sets with west-east orientation, related to the early Jurassic

Neuquén Basin rifting phase, including Penitentes, El Humazo, Covunco, and El Cajon faults (Galetto et al., 2018), intersects and segments the Manchana Covunco fault (Figure 1) (Mariot, 2008).

IV. DATA AND METHODOLOGY

The seismological data used in this paper, correspond to two different time periods. The first time period comprises continuous data from March to April 2019, when the largest registered earthquake occurred in the Domuyo region. The stations used are from Instituto Geofísico Sismológico Ing. Volponi (IGSV) from San Juan University, Centro Sismológico Nacional from Chile University (CSN, Introducción | Centro Sismológico Nacional (uchile. cl)) and from the Federation of Digital Seismograph Networks (FDSN) (Figure 1B). For the second period, data was registered from December 2019 to January 2021 and were obtained from a local seismological experiment by IGSV, which deployed eight broadband seismological stations around the Domuyo volcanic complex (Figure 2 and Table 1). Also, additional, stations located in Neuquén and Mendoza Provinces by IGSV, and in Chile from available data in the FDSN network and were used during this last period. To identify automatically the seismicity of the area, we used the SeisComP3 software (Helmholtz Centre Potsdam GFZ German Research Centre for Geosciences and gempa GmbH, 2008), which was configured to detect events greater than 1.8 magnitude, observed in at least six stations.

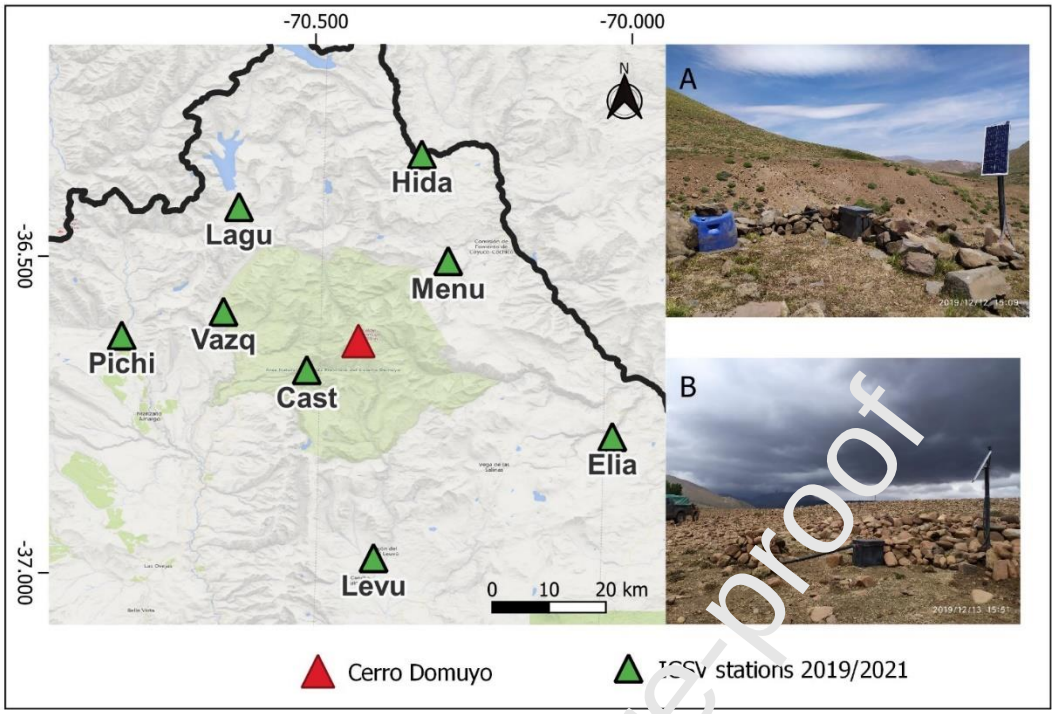

Figure 2. Satellite image of the study zone and the local seismological network with green triangles. A) VAZQ station figure, which shows a solar panel, a register in the grey box, and a sensor in the blue container. B) LEVU station figure, with characteristics similar to the previous one, except that the sensor is covered with rocks and container.

STATION	***Sensor***	***Register***	***Longitude (°)***	***Latitude (°)***	***Elevation (m)***	***VPP (Volt)***	***Samples per second***
Lagu	6T	Minimus	-70,621	-36,422	1953	20.5	200
Cast	120PA	Centaur	-70,514	-36,680	2480	10	200
Vazq	120PA	Taurus	-70,645	-36,58	1613	16	200
Pich	TC-120	Centaur	-70,806	-36,625	1376	20	200
Levu	6T	Minimus	-70,408	-36,972	1352	20.5	200
Elia	120PA	Centaur	-70,031	-36,785	1580	20	100
Hida	6T	Minimus	-70,332	-36,339	1615	20.5	200

Menu	120PA	Centaur	-70,29079	-36,50781	1788	20	200

Table 1. Equipment, location, and configuration details of the eight stations installed in the local Domuyo experiment.

After events detection, the waveform data from different networks were integrated into a unique 1-hour archive in a miniseed format and organized in the Seisan database (Havskov and Ottemoller 2010). The instrumental station response was obtained from the software Portable Data Collection Centers (PDCC), the Incorporated Research Institutions for Seismology (IRIS). We used Hypocenter (Lienert and Havskov, 1995) to obtain the location parameters considering the 1D velocity model from Bohm et al. (2002). The local magnitude (Ml) was obtained for each vertical component (and then averaged) in semi-automatic mode from the S wave maximum amplitude in the Seisan platform. The coda duration is proportional to the size of the earthquake, although it can be affected by other factors, such as the soil conditions in which the station is located (Suteau and Whitcom, 1979). Nevertheless, in cases where Ml could not be calculated, the coda magnitude was obtained from the seismic record in the Seisan platform.

The focal mechanism solution was obtained from the polarity of the first P wave motion using FOCMEC (Snoke et al., 1984). A reliable mechanism solution is subject to good station coverage. Azimuthal´s gap larger than 90° can introduce instabilities in the focal mechanism solutions (Hardebeck and Shearer, 2002). For such reason, data was thoroughly completed using all stations of the different available networks (IGSV, CSN, and FDSN). All focal mechanism solutions were determined by allowing less than one inconsistent polarity; solutions were rejected when the number of polarity inconsistencies (compressions or dilations located in quadrants of opposite polarity) exceeded a predetermined maximum. According to the event, we calculated the focal mechanism with grid search (GRS) from 5° to 10°.

V. RESULTS

Local Seismicity in the Domuyo

The seismicity presented in this work belongs to three different periods, the first period (only 1 event) from September 2016, the second is March to April 2019, and the third period from December 2019 to January 2021, using different combinations of seismological data (Figure 3a and Figure 4a). In our interpretations, we also reference to the volcano-tectonic events in Domuyo region published in Godoy et al. (2021), and to the seismicity from IGSV catalog in the 2010 to 2020 period.

The first records of crustal seismicity detected by INPRES (Instituto Nacional de Prevención Sísmica) at Domuyo was the Ml 3.3 10 September 2016 event. We present the relocated earthquake in Table 2. Given the distribution of the networks that recorded it, which are far from the area we can not accurately calculate the depth, but we could calculate the focal mechanism. The focal mechanism presents two possible solutions a thrust solution with a strike component (Figure 3, events 0-A and Table 2, Appendix Figure A), and other normal solution with a strike component (Figure 3, events 0-B and Table 2, Appendix Figure A).

The largest event reported in the Domuyo region occurred on March 27th , 2019 and had a magnitude of 4.4 (NEIC – USGS). We relocated this event to improve its location parameters. Table 3 shows the earthquake parameters in the location from in the USGS catalog and the new parameters (much lower azimuthal GAP) (Figure 4). Interestingly, the most important feature observed is its occurrence at a different depth, 3.9 km instead of 10 km.

We visualized the continuous database from March to April 2019 with only five crustal events (depth shallower than4.8 km) with coda magnitude from 1.4 to 2.4. Only the event of Ml 4.4 had a reliable

focal mechanism, presenting a normal solution with a small strike component. The focal mechanism solution (Figure 4, Table 2, and Appendix Figure B) shows approximately WSW-ENE nodal planes dipping to the SE (PN1) and the NW (PN2).

In this work, using the network installed in the DVC from December 2019 to January 2021, we only selected events with a magnitude greater than Ml 1.8, which were quickly and automatically detected. The detected events show magnitudes Ml between 1.9 to 2.8, and a shallow focal depth, between 1.8 and 5.2 km, similar to the depth obtained for the Ml 4.4 March 2019 event. In Figure 3, the focal mechanisms with reliable solutions of shallow events are plotted and Table 2 shows their parameters. The event of 3 January 2020, with a magnitude of Ml 2.3, presents a normal solution with a strike component (Figure C in Appendix). On the other hand, the events of 2 and 22 May (Appendix Figure D and Figure E, respectively), with a calculated Ml of 2.8, present normal solutions with a small strike component. It is remarkable the similarity of the focal mechanism solutions of events 1, 2, 3, and 4 (see Table 2), all with their nodal planes approximately W-E, dipping PN1 ~ to the south (average 47°) and PN2 ~ to the north (average 44°). Finally, the event of 8 September 2020, with a magnitude of 1.9 and the shallowest depth of 1.8 km, presents a single solution (Figure 5 and appendix Figure F). This event presents NNE-SSW nodal plane (PN1) dipping to the southeast and NNW-SSE nodal plane 2 dipping to the SW.

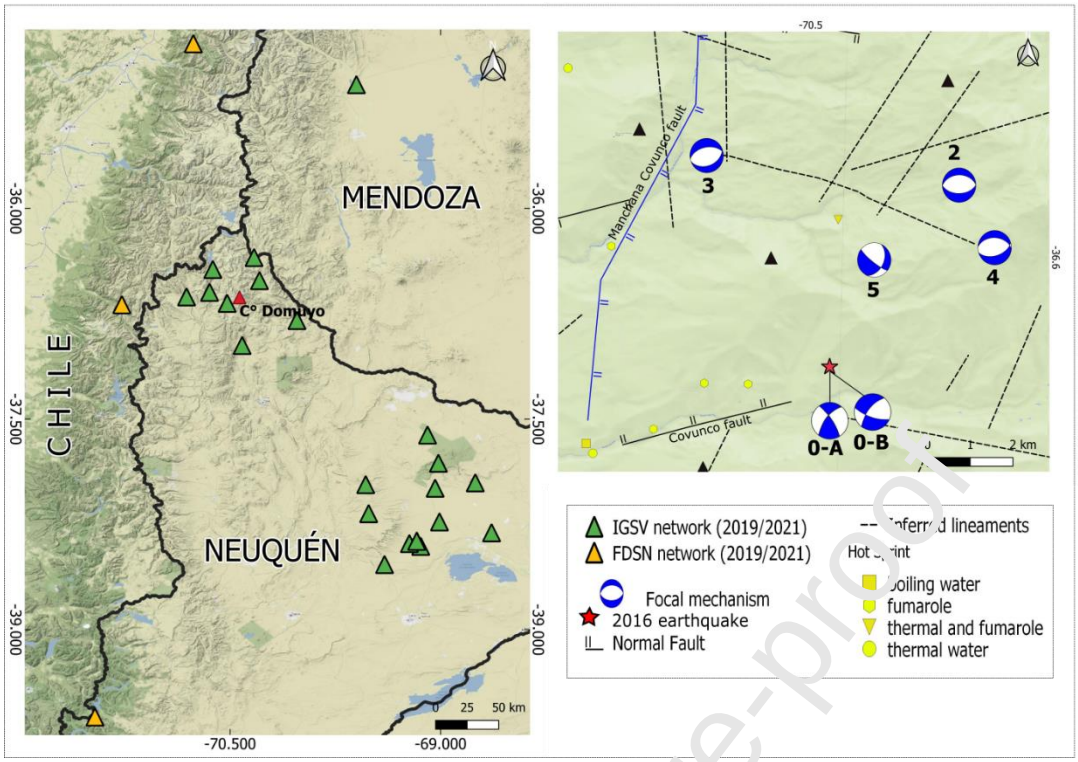

Figure 3. In the left image, the green triangles represent the IGSV station locations, and the orange triangles the FDSN station (from Centro Sismológico Nacional, Universidad de Chile) locations used to calculate the focal mechanism corresponding to the 2020 events. On the right, the focal mechanism solutions are plotted in their locations. Each mechanism has a number to identify it in Table 2.

ID	Month_Day_Year	HRMM_Sec	Latitude	Longitud	Prof.	NSTA	Ml	RMS	GAP	NPol	GRS	Rb/Bz/Des	Plane
0	09_10_2016	1122_2.5	-36.673	-70.496	0	19	3.3*	0.41	153	16	10	221/56/156	**PN1-A**
												325/71/36	**PN2-A**
												221/56/156	**PN1-B**
												107/66/-32	**PN2-B**
1	03_27_2019	2027_29.3	-36.616	-70.366	3.7	52	4.4*	0.7	81	18	5	85/45/-83	**PN1**
												255/45/-97	**PN2**
2	01_03_2020	1150_35.3	-36.632	-70.469	5.2	25	2.6	0.9	77	15	10	89/50/-90	**PN1**
												269/40/-90	**PN2**
3	05_02_2020	2119_32.2	-36.628	-70.522	4.2	24	2.8	1.0	9[illegible]	[illegible]2	10	69/40/-98	**PN1**
												259/50/-83	**PN2**
4	05_22_2020	1731_1.3	-36.665	-70.463	3.6	25	2.8	1.[illegible]	81	16	10	73/51/-103	**PN1**
												273/41/-75	**PN2**
5	09_08_2020	1955_11.1	-36.658	-70.475	1.8	13	1.9	0.9	90	9	5	25/42/-17	**PN1**
												128/79/-131	**PN2**

*Table 2. Events with focal mechanism solutions, which were obtained in this research. The table indicates the event identification number (ID), location parameters, number of stations used (NSTA), magnitude (Ml), root mean square residual (RMS), the maximum angle where there is no station coverage (GAP), reading number of first arrivals with identified polarity (NPol), grid search (GRS) *Magnitude from NEIC Catalog. Strike, dip, and rake for each nodal plane according to the convention of Aki and Richards (1980).*

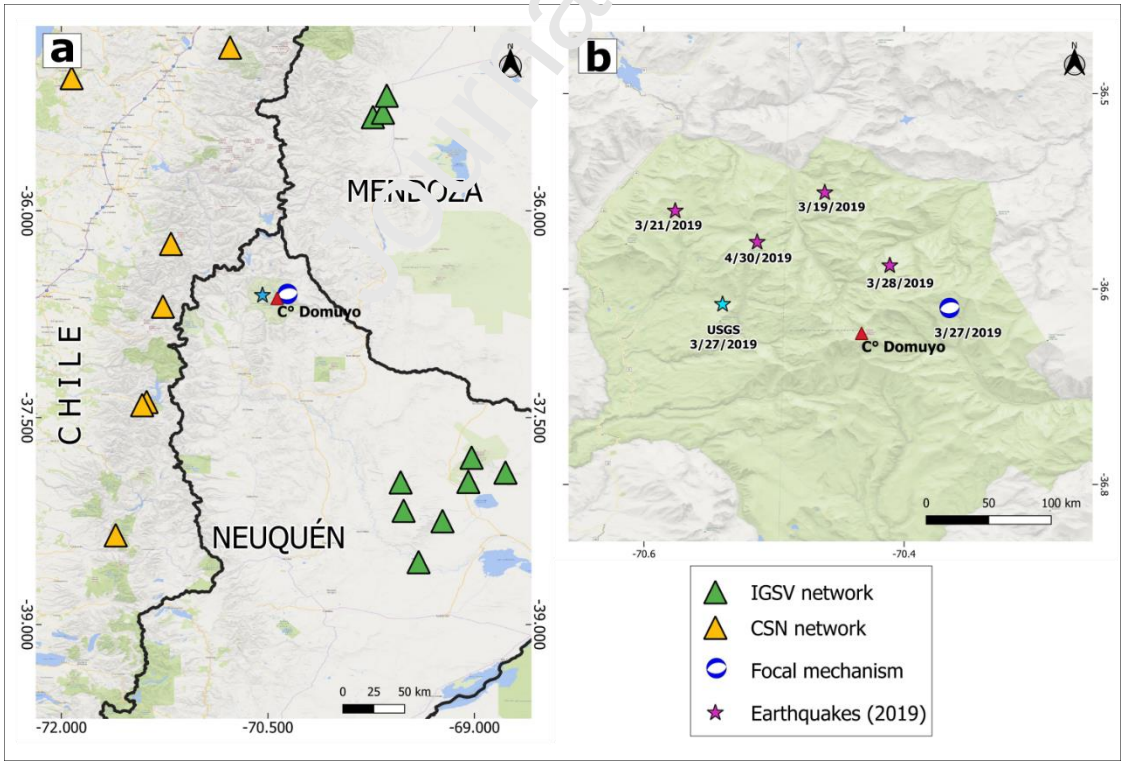

Figure 4. a) Image of the location of the seismological stations. Green and orange triangles are the IGSV stations and CSN stations, respectively. The red triangle shows the Cerro Domuyo. The light blue star shows the 27 March 2019 epicenter from NEIC Catalog and the beach ball in blue color shows the focal mechanism solution obtained in this work for this event. b) Amplified region shows the 27 March 2019 epicenter (USGS), the new location 20 km to the east (at the beach ball position) including foreshock and aftershock events.

Source	Latitude (°)	Longitude (°)	Depth (km)	Local Magnitude (Ml)	Gap
NEIC -USGS	-36.611	-70.539	10	4.4	151
This research	-36.616	-70.366	3.9	-	81

Table 3. Location parameters for the earthquake of 27 March 2019 from the NEIC Catalog (USGS) and from this research.

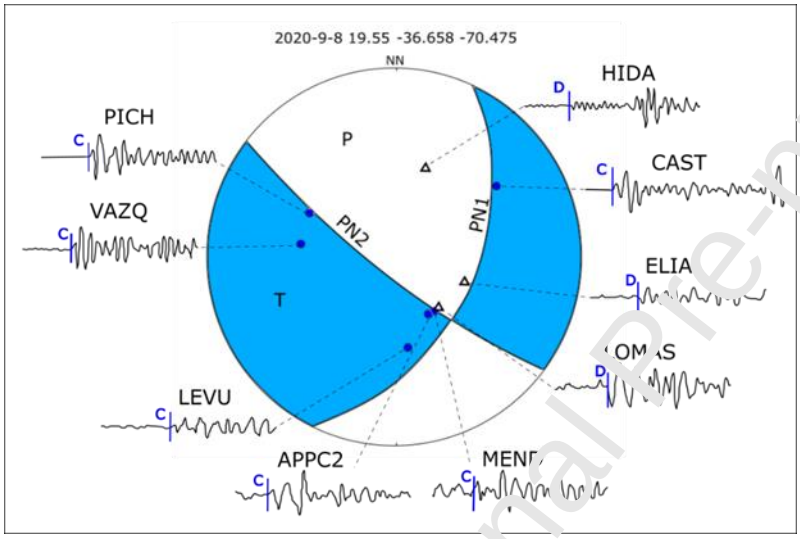

Figure 5. Focal mechanism solution that belongs to event #5. The waveform of the first P wave arrivals at each station is picked and classified according to whether it is distensive (D) or compressive (C). The distensive and compressive movements are plotted with white triangles and blue circles in the stereographic representation. The solutions found are two nodal planes represented by continuous lines marked by PN1 and PN2.

VI. INTERPRETATION AND DISCUSSION

I. Interpretation of local seismicity and focal mechanism solutions

To understand the seismic potential of structures affecting the Domuyo volcanic complex (DVC), we used local and regional seismological networks. We calculated focal mechanism solutions, which showed mostly the activity of normal faults with a small strike-slip component. In particular, the earthquake of March 27th, 2019 (focal mechanism 1 in Figure 6 and Table 2) is located on the eastern

flank of Domuyo, in coincidence with E – W structures. However, this event (and events 2, 3, and 4, see Table 3 and Figure 6) could be associated with normal E -W structures (e.g. Humazo) or with a structure inferred by satellite gravimetric data (Godoy, 2022). Considering there is no available geological data to constrain, it is not possible to determine which of those nodal planes constitutes the fault plane.

In the local experiment carried out in DVC (Figure 2), we calculated 4 focal mechanisms, 3 of them had a normal solution (with a small strike-slip component) with approximately east-west nodal planes (events located at similar depths and with similar Ml) (see events 2, 3, and 4 in Table 2). The other event occurred on 8 September 2020 (Table 2), was located at a shallower depth, and had a lower magnitude, presenting a strike-slip solution with a normal component and nodal planes oriented in NNE-SSW and NW -SE directions. In the event 3 (2 May 2020 earthquake), given its proximity to the El Humazo fault (due to a location uncertainty of approximately 3 km), we assume that this mechanism could represent an event associated with this southeast-dipping normal fault (PN1 has been chosen as the fault plane). We consider that this structure is the source of the high shallow seismicity registered in 2015/2016 (Godoy et al., 2021). However, we also analyzed the mechanism solution of this event together with events 2 (3 January 2020) and 4 (22 May 2020). Therefore, these solutions probably belong to a structure inferred by other authors (Pesce, 1987; Mariot, 2008; Galetto et al., 2018). Consequently, we defined it as a normal fault, with an approximate E -W direction of both fault planes. As we have no prior field evidence, we were unable to select a nodal plane as the fault plane.

The focal mechanism of the 8 September 2020 earthquake (Number 5, Figure 6) corresponds to another fault system, a strike-slip type with normal components (appendix Figure F). In this work, we assumed that the Nodal Plane 1 (PN1) was the most suitable, fault plane, considering the trend of the

photo-interpreted structures (Galetto et al., 2018) with a northeast-southwest orientation, such as the one located in the Cerro Domo area. Additionally, Galetto and co-authors (2018) carried out kinematic measurements in the fault planes of the Manchana Covunco Fault, in the homonymous stream and nearby areas, and identified normal dextral kinematic displacements and two planes of NNE and NNW fault solutions. We conclude that the results obtained by Galetto and co-authors (2018) and those obtained from seismological data in this work (with greater depths) correspond to the same family of faults with a NNE- SSW orientation, marked as inferred lineaments/structures in Figure 6.

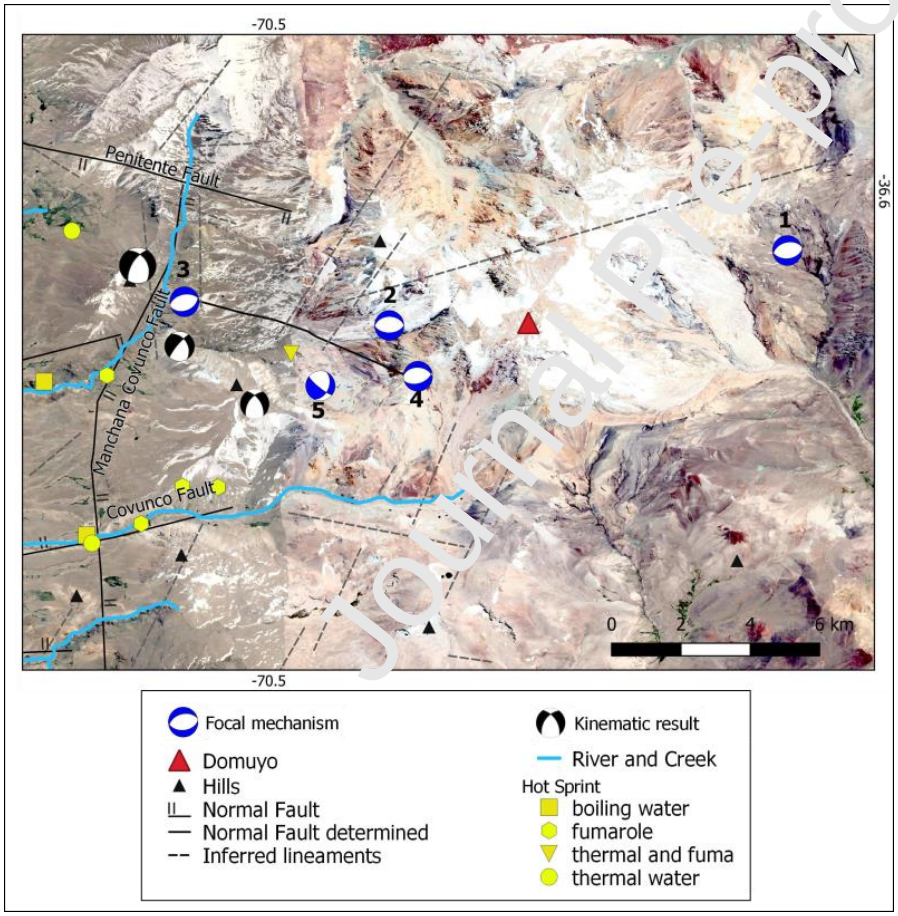

Figure 6. Satellite image with the results of the focal mechanism. The normal fault determined by mechanisms 1, 2, 3, and 4 is plotted. The focal mechanism solution of the 8 September 2020 earthquake, is compared with the kinematic results of Galetto et al. (2018).

II. Ten-year seismological evolution of the Domuyo Volcanic Field

In order to assess the long-term evolution of the seismic activity in DVC, we first searched the available earthquake IGSV catalog for information about seismicity in the area, including events with a magnitude greater than 2. This catalog comprises events that occurred from 2010 to 2020 when the local IGSV networks in the nearest Domuyo region (south of Mendoza Province and north of Neuquén Province; Figure 1) were operating. In Figure 7, we plotted the detected earthquakes with circles, characterizing each year with a different color. The histogram shows that the Domuyo region was seismically inactive in the 2010-2015 period, with no evidence of earthquakes with a magnitude over 2, so we can consider the DVC as a zone of reduced seismicity around 2016. Seismicity begins to be detected in 2016 (according to the regional catalog, see Figure 1), with a maximum peak of "tectonic" events observed in 2017-2018, decreasing then until 2020. This becomes more evident if we refer to global (NEIC-USGS) and regional (INPRES) catalogs, which have been characterized as a reduced seismicity zone since 1973 (until 2019) and 1999 (until 2016), respectively (see Figure 1C). Additionally, from December 2015 to March 2016 a local network detected a large number of volcano-tectonic events with magnitudes Ml less than 1.2 in the Domuyo region (Godoy et al., 2021).

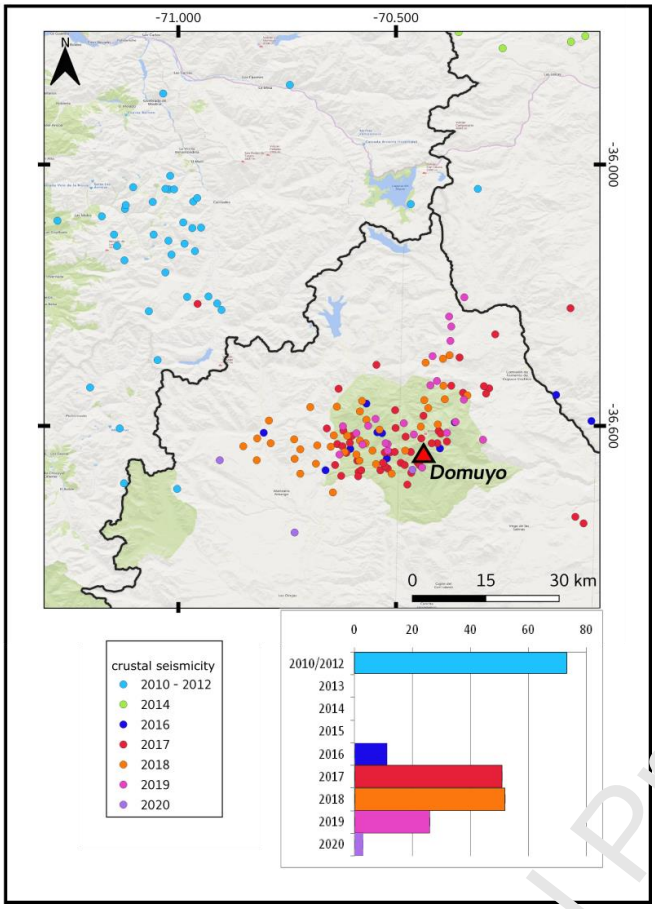

Figure 7. Location of the crustal earthquakes in the study area from data obtained by the IGSV local-temporal seismological networks. The histogram represents the number of earthquakes that occurred per year. Different colored circles mark the earthquake epicenters per year. Note that from 2016 to 2020, an increase in crustal seismicity is observed in the study area.

Based on the obtained results a clear temporal and spatial relationship is observed between crustal seismicity and VT events in relation to detected inflation, described neotectonic deformations, and surficial warming (Galetto et al., 2018; Lundgren et al. 2018; Astor et al., 2019; d'Oreye et al., 2019, Lundgren et al., 2020). In particular, Lundgren et al. (2020), from a crossed correlation analysis applied to the INSAR and TIR temporal series propose three possible models to explain Domuyo´s behavior from 2008 to 2019. In particular, in Model 3, the Authors propose that magma injection at shallower levels (evidenced by surficial deformation since mid-2014) leads to gas transfer processes from the reservoir to the surface (evidenced by surficial warming from approximately mid-2017).

From the focal solution mechanisms associated to the measured crustal events, it is evident that at least from September 2016 (two years later than the beginning of the inflation process), the DVC is submitted to extensional-transtensional deformation. Crustal seismicity presents a higher peak around 2017/18. In particular, higher magnitude earthquake in 2019 locates on the eastern slope of the DVC, showing that the entire system was subject to extension. Extensional crustal seismicity continues up to 2020 concentrated beneath the western volcanic slope near the Humazo Fault where most VT events occurred. Since 2020 seismicity has decreased in accordance with a stabilization of the vertical deformation. This seismic sequence agrees with the proposal of a degasification process associated with the emplacement of a magmatic body at shallow depth, evidenced by the inflation described in Lundgren et al. (2020).

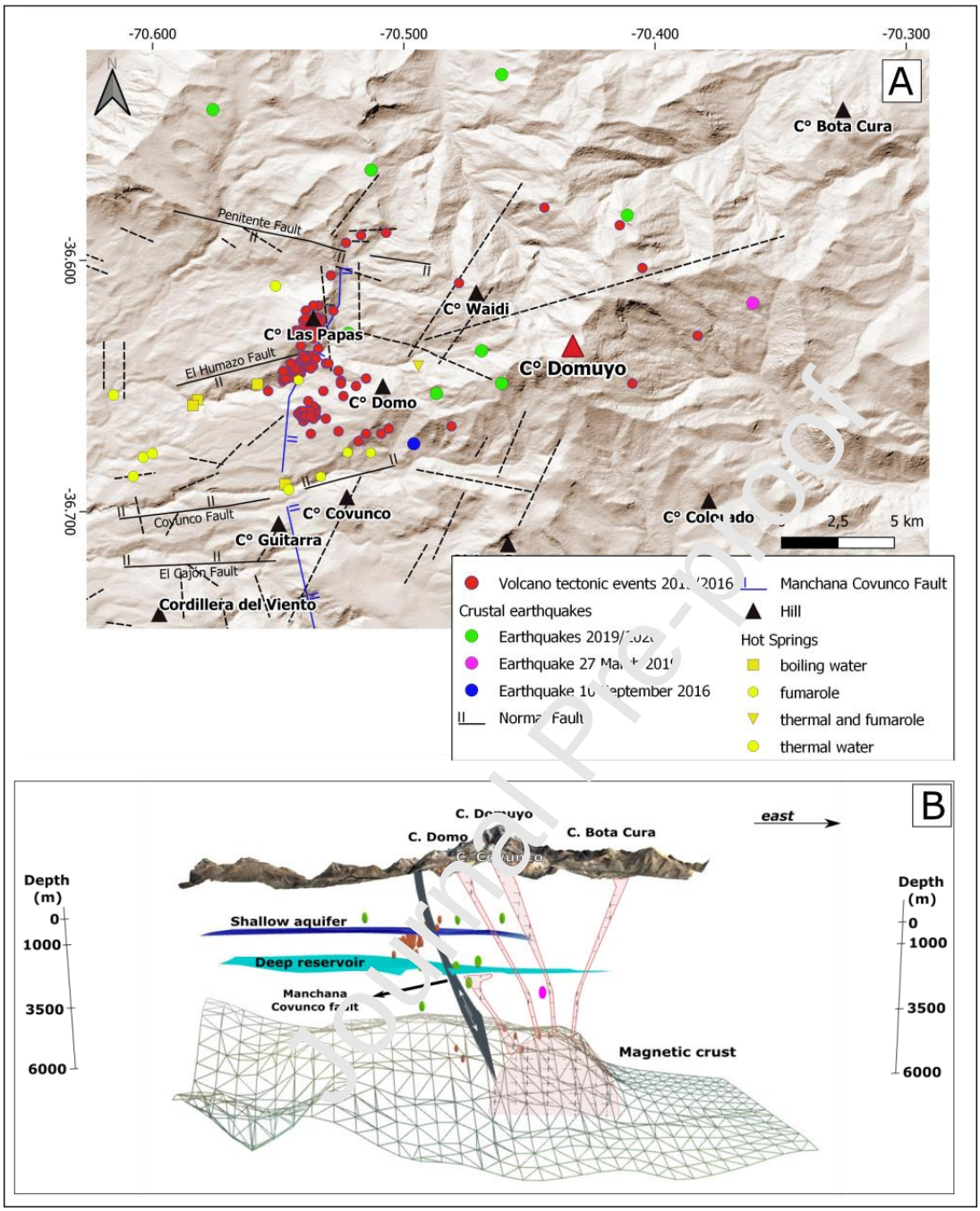

Figure 8. A- -DEM showing the principal volcanic centers that form the DVC with black triangles. The hot springs are indicated with yellow color and the active normal faults with black lines. The crustal earthquakes and volcano-tectonic (VT) epicenters are shown with different colored circles (the VT events are as described by Godoy et al., 2021). B- A summary model, the magmatic chamber is observed at a depth of approx. 6,5 km (Lundgren et al., 2020) where the magnetic crust is shallower. The new magmatic pulse is close to the Manchana Covunco fault. The seismicity is plotted with colored ovals as in the description of the map above. 3D representation made with Andino 3D (Cristallini et al., 2019).

VII. CONCLUSIONS

In this work, we re-located the first seismic crustal event since 1973 that were registered in 2016. Additionally, we re-located the higher magnitude event in 2019 in the area. For both events we calculated the first focal mechanisms yielding extensional deformations plusstrike-slip components. Four additional focal mechanisms yielding extensional deformations were added following the seismic sequence of 2019/21. These extensional-transtensional events coincide with neotectonic deformations mainly concentrated beneath the western slope of the . Therefore, based on the data released by Lundgren et al. (2018, 2020) and the data obtained in this work, we infer that the DVC from 2016-2020 was subject to an extensional deformation most likely associated with the degasification of a shallow magmatic body that promoted surficial warming, delayed 2.7 years with respect to the beginning of the inflation process.

VIII. ACKNOWLEDGMENTS

The authors are grateful to FONCYT for funding the studies through Projects PICT 2017-1252, to the National San Juan University and to CONICET. We would like to extend our gratitude to the facilities of IRIS Data Services, and specifically the IRIS Data Management Center, which provided some waveforms used in this study. IRIS Data Services are funded through the Seismological Facilities for the Advancement of Geoscience (SAGE) Award of the National Science Foundation under Cooperative Support Agreement EAR-1851048.s. Thanks to Dr. Diana Comte from the University of Chile and a Instituto Nacional de Prevención Sismica (INPRES) de Argentina for sharing the seismological station network data, and Dr. Caselli Alberto, a volcanologist who is one of the pioneers in studying the Domuyo through multidisciplinary studies. The 2019/2021 local network was installed thanks to the support and accompaniment of Hector Valdez (park ranger in Varvarco), Braian Bravo and Ramón Fernandez (policemen in COCHICO), Marta Fuenzalida (principal of School N° 236 in Pichi, Neuquén), Muñoz, Jorqueda, Quiroz, Hidalgo, Vera and their families. They provided us with shelter while this project was being carried out.

IX. REFERENCES

Aki, K., and Richards, P.G., 1980. Quantitative Seismology. W. H. Freeman, New York.

Astort, A., Walter, T. R., and Ruiz, F. 2019. Unrest at Domuyo Volcano, Argentina, Detected by Geophysical and Geodetic Data and Morphometric Analysis: 1–28.

Bohm, M., Lüth, S., Echtler, H., Asch, G., Bataille, K., Bruhn, C., Rietbrock, A., and Wigger, P., 2002. The Southern Andes between 36◦ and 40◦S latitude: seismicity and average seismic velocities. Tectonophysics 356, 275–289. https://doi.org/10.1016/S0040- 1951(02)003992.

Borghi, P., Fennell, L., Omil, R. G., and Folguera, A., 2023. Multiple phases of deformation that shaped the southern Central Andes (36.5° S) from crosscutting relationships with Cenozoic backarc magmatism. Journal of Geodynamics, 156, 101970.

Brousse, R., and Pesce, A. H., 1982. Cerro Domo: Un volcán Cuartario con posibilidades geotermicas. Provincia del Neuquén. In Proceedings, 5th Congreso Latinoamericano de Geología: Buenos Aires. Servicio Geológico Nacional, Subsecretaria de Minería (Vol. 4, pp. 197-208).

Chiodini, G., Liccioli, C., Vaselli, O., Calabrese, S., Tassi, F., Caliro, S., Caselli, A., Agusto, M., and D'Alessandro, W. 2014. The Domuyo volcanic system: An enormous geothermal resource in Argentine Patagonia. Journal of Volcanology and Geothermal Research, 274: 71–77. Elsevier B.V.

Collettini, C., and Sibson, R. H. 2001. Normal faults, normal friction? Geology. doi: 10.1130/0091-7613 vol. 29, no. 10, p. 927-930.

Cristallini E., Hernández R., Balciunas D., Nigro J., Dellmans M., Costilla M. (2019). Andino 3D: structural modeling software (Version 2.0.3.3). CONICET-LATE ANDES [Software]. Available from http://www.andino3d.com.ar/.

d'Oreye N., Derauw D., Libert L., Samsonov S., Dille A., Nobile A., Monsieiurs E., Dewitte O., and Kervyn F., 2019. Automatization of InSAR mass processing using CSL InSAR Suite (CIS) software for Multidimensional Small Baseline Subset (MSBAS) analysis: example combining Sentinel-1 and Cosmo-Sky Med SAR data for landslides monitoring in South Kivu, DR Congo. Abstract, 13-17 May 2019, ESA Living Planet Symposium 2019, Milano, Italy - Samsonov, S., A.

Farías, M., Comte, D., Charrier, R., Martinod, J., David, C., Tassara, A., Tapia, F., and Fock, A., 2010. Crustal-scale structural architecture in central Chile based on seismicity and surface geology: Implications for Andean Mountain building. Tectonics, 29(3). https://doi.org/10.1029/2009TC002480

Folguera, A., Ramos, V.A., Zapata, T., and Spagnuolo, M., 2007. Andean evolution and deformational mechanisms at the Guañacos and Chos Malal fold and thrust belts (36º30´-37ºS). Journal of Geodynamics. GEOD 2006-02. doi: 10.1016/ j.jog.2007.02.003, 44: 129-148.

Galetto, A., García, V., and Caselli, A., 2018. Structural controls of the Domuyo geothermal field, Southern Andes (36°38'S), Argentina. Journal of Structural Geology, 114: 76–94. Elsevier Ltd.

Godoy, L. B., Nacif, S., Lupari, M., García, H. P., Correa-Otto, S., Melchor, I., Pechuan, S., Ariza, J., Gimenez, M. E. and Caselli, A. T., 2021. Geophysical evidence of first stages of inflation in Domuyo volcanic center in northwestern Neuquén province, Argentina. Journal of South American Earth Sciences; 107; 102694.

Godoy, Laura Beatriz. (2022). Evidencia y análisis de cambios temporales en la zona del cerro Domuyo. Caracterización geofísica de su campo geotermal, y su microsismicidad asociada. Tesis doctoral. Universidad Nacional de Río Negro, http://rid.unrn.edu.ar/handle/20.500.12049/10190.

Groeber, P., 1947. Hojas Domuyo, Mari Mahuida, Huahuar Co y parte de Epu Lauquen. En Observaciones Geológicas a lo largo del Meridiano 70, 75–136.

Hardebeck, J. L., and Shearer, P. M., 2002. A new method for determining first-motion focal mechanisms, Bull. Seismol. Soc. Am., 92, 2264–2276.

Havskov, J., and Ottemöller, L.: Location. In: Havskov, J., 2010. (ed.) Routine Data Processing in Earthquake Seismology: With Sample Data, Exercises and Software, pp. 101–149. Springer, Dordrecht https://doi.org/10.1007/978-90-481-8697-6_5.

Helmholtz Centre Potsdam GFZ German Research Centre for Geosciences and gempa GmbH, 2008. The SeisComP seismological software package. GFZ Data Services. doi:10.5880/GFZ.2.4.2020.003.

JICA, 1983. Interim Report on the Northern Neuquén Geothermal Development Project. First-Second Phase Survey. Japan International Cooperation Agency-Ente Provincial de Energía de la Provincia de Neuquén (unpublished), Neuquén, p. 85.

JICA, 1984. Final Report on the Northern Neuquén Geothermal Development Project. Third Phase Survey. Japan International Cooperation Agency-Ente Provincial de Energía de la Provincia de Neuquén (unpublished), Neuquén, p. 105.

Leanza, H.A., Llambías, E.J., and Carbone, O., 2005. Unidades estratigráficas limitadas por discordancias en los depocentros de la cordillera del Viento y la sierra de Chacaico durante los inicios de la cuenca Neuquina. Congreso de exploración de hidrocarburos.6.

Lienert, B. R. E., and Havskov, J., 1995. A computer program for locating earthquakes both locally and globally. Seismological Research Letters. 66:26–36.

Llambías, E. J., Leanza, H. A., y Carbone, O. 2007. Pérmico Al Jurásico Temprano En La Cordillera Geológicas Y Geoquímicas Del Inicio De La. Revista de la Asociación Geológica Argentina, 62: 217–235.

Llambías, E.J., Danderfer, J.C., Palacios, M., y Brogioni, N., 1978. Las rocas ígneas cenozoicas del Volcán Domuyo y áreas adyacentes. 7° Congreso Geológico Argentino, Actas (2): 569-584, Neuquén.

Lundgren, P., Girona, T., Samsonov, S., Realmuto, V., and Liang, C., 2018. Under the radar: new activity beneath the·roof of Patagonia", Domuyo volcano, Argentina. In: AGU Fall Meeting 2018. AGU.

Lundgren, P., Girona, T., Bato, M. G., Realmuto, V. J., Samsonov, S., Cardona, C., Franco, L., Gurrola, E., and Aivazis, M., 2020. The dynamics of large silicic systems from satellite remote sensing observations: the intriguing case of Domuyo volcano, Argentina. Scientific Reports, 10: 1–15. Nature Publishing Group UK.

Mariot, M. C., 2008. Geología Y Estructura Del Cerro Domuyo, Provincia De Neuquén. Degree thesis (unpublished). University of Buenos Aires, 154.

Miranda, F., Folguera, A., Leal, P. R., Naranjo, J. A., y Pesce, A. H., 2006. Upper Pliocene to Lower Pleistocene volcanic complexes and upper Neogene deformation in the south-central Andes (36°30'-38°S). Special Paper of the Geological Society of America, 407: 287–298.

Pesce, A.H., 1987. Evaluación Geotérmica del Área Cerro Domuyo: Síntesis Estratigráfica, Vulcanológica, Estructural y Geoquímica - modelo Geotérmico Preliminar, provincia del Neuquén, República Argentina. In: Proceedings International Meeting on Geothermics and Geothermal Energy, vol. 5. Revista Brasileira de Geofísica, Sao Paulo, Brazil, pp. 283–299.

Pesce, A.H., 2013. The Domuyo geothermal area, Neuquén, Argentina. Geothermal Resources Council 37, 309-314.

Silva-Fragoso, A., Ferrari, L., Norini, G., Orozco-Esquivel, T., Corbo-Camargo, F., Bernal, J. P., Castro, C., and Arrubarrena-Moreno, M., 2021. Geology and conceptual model of the Domuyo geothermal area, northern Patagonia, Argentina. Journal of Volcanology and Geothermal Research, 420: 107396. Elsevier B.V.

Snoke, J. A., Munsey, J. W., Teague, A. G. and Bollinger, G. A. 1984. A program for focal mechanism determination by combined used of polarity and SV-P amplitude ratio data, Earthquake Notes 55, p. 15

Stern, C. R., 2004. Active Andean volcanism: its geologic and tectonic setting Andean Geology. Servicio Nacional de Geología y Minería. Santiago, Chile, 31 (2), 161-206.

Suteau, A. M., and Whitcomb, J. H., 1979. A local earthquake coda magnitude and its relation to duration, moment Mo, and local Richter magnitude ML. Bulletin of the Seismological Society of America, 69(2), 353-368.

Tassara, A., and Yáñez, G., 2003. Relación entre el espesor elástico de la litosfera y la segmentación tectónica del margen andino (15°-47°S). Revista geológica de Chile, 30 (2), 159-186.

Tassi, F., Liccioli, C., Agusto, M., Chiodini, G., Vaselli, O., Calabrese, S., Pecoraino, G., Tempesti, L., Caponi, C., Fiebig, J., Caliro, S., and Caselli, A., 2016. The hydrothermal system of the Domuyo volcanic complex (Argentina): A conceptual model based on new geochemical and isotopic evidences. Journal of Volcanology and Geothermal Research, 328: 198–209.

Zappettini, E.O., Chernicof, C.J., Santos, J.O.S., Dalponte, M., Belousova, E., and Mc Naughton, N., 2012. Retro wedge-related Carboniferous units and coeval magmatism in the northwestern Neuquén province, Argentina. Int. J. Earth Sci. 101, 2083–2104.

Zöllner, W. y Amos, A.J., 1973. Descripción geológica de la Hoja 32 b Chos Malal, provincia del Neuquén. Servicio Nacional Minero Geológico, Boletín 143: 1-91, Buenos Aires.

Godoy, Laura B. analyzed seismological data, conceived of the presented result interpretation, and wrote the original draft. Nacif, Silvina, contributed to the interpretation of the results and setting carried out a manuscript critical revision, and help to co-wrote the manuscript, together with Gimenez, Mario and Folguera, Andrés.

Nacif, Andrés, designing computer programs, and collaborate in the seismological network installation.

Christiansen, Rodolfo, and Álvarez, Orlando collaborated in the seismological network installation and contributed to data quality discussions.

Gimenez Mario and Nacif Silvina Acquisition of the financial support for the project leading to this publication.

The authors of this work declare that it is an original article, that it has not been sent to another journal, and that there are no conflicts of interests

- First focal mechanisms in Domuyo Volcanic Complex (DVC), with principally normal solution.
- DVC from 2016-2020 was subject to an extensional deformation.
- This deformation is associated with the degasification of a shallow magmatic body.